

Supramolecular Structures Formed by Calix[8]arene Derivatives

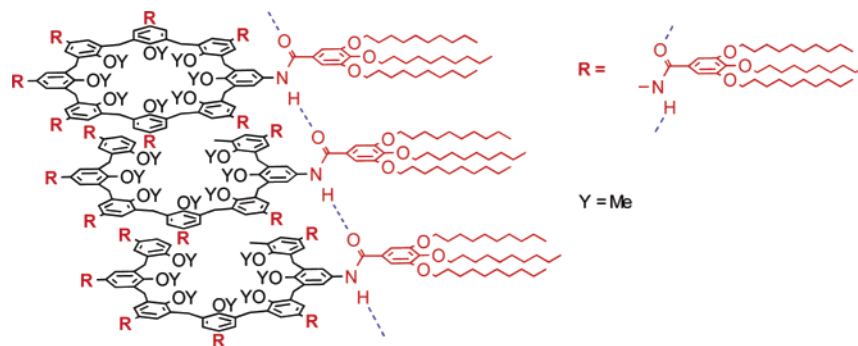
Ganna Podoprygorina,[†] Jian Zhang,[‡] Vasilij Brusko,^{†,§} Michael Bolte,^{||}
Andreas Janshoff,^{*,†} and Volker Böhmer^{*,†}

Abteilung Lehramt Chemie, Fachbereich Chemie und Pharmazie,
Johannes Gutenberg-Universität, Duesbergweg 10-14, D-55099 Mainz, Germany,
Institut für Physikalische Chemie, Fachbereich Chemie und Pharmazie,
Johannes Gutenberg-Universität, Welderweg 11, D-55099 Mainz, Germany, and
Institut für Organische Chemie, Johann Wolfgang von Goethe Universität,
Marie Curie-Strasse 11, D-60439 Frankfurt/Main, Germany

vboehmer@mail.uni-mainz.de; janshoff@mail.uni-mainz.de

Received October 28, 2003

ABSTRACT



Octamethoxy calix[8]arenes substituted in the para position by amide, urea, and imide functions were synthesized from the octamethyl ether of *tert*-butylcalix[8]arene by ipso nitration, reduction, and acylation. Scanning force microscopy of spin coated samples on graphite suggests that these derivatives self-organize into tubular nanorods via hydrogen bonds between *p*-amide functions. A single-crystal X-ray structure reveals a centrosymmetric conformation for the octanitro derivative.

Calix[8]arenes are easily available in one-pot syntheses by condensation of *p*-alkyl phenols with formaldehyde under alkaline catalysis.^{1,2} Although the yield for the *tert*-butyl calix[8]arene (62–65%) is higher than for *tert*-butyl calix[4]arene (50%), the chemistry of calix[8]arenes³ is far less developed than for calix[4]arenes. While the complete debutylation (transbutylation) has been known for a long

time,⁴ octabromo and octaiodo derivatives were described only recently.⁵ They were used in cross-coupling reactions of the Sonogashira,⁵ Negishi,⁶ and Suzuki type.⁶

In their so-called “pleated loop conformation”, stabilized by intramolecular hydrogen bonds, calix[8]arenes provide a cavity with an internal diameter of 0.7–0.8 nm as shown by X-ray crystallography.⁷ ¹H NMR spectra in, e.g., CDCl₃

[†] Abteilung Lehramt Chemie, J. G.-Universität, Mainz.

[‡] Institut für Physikalische Chemie, J. G.-Universität, Mainz.

[§] Permanent address: Chemical Department, Kazan State University, Kremlevskaya St. 18, 420008 Kazan, Russia.

^{||} J. W. Goethe Universität, Frankfurt/Main.

(1) For reviews see: *Calixarenes 2001*; Asfari, Z., Böhmer, V., Harrowfield, J., Vicens, J., Eds.; Kluwer Academic Publishers: Dordrecht, 2001.

(2) Gutsche, C. D. Synthesis of Calixarenes and Thiacalixarenes. In *Calixarenes 2001*; Asfari, Z., Böhmer, V., Harrowfield, J., Vicens, J., Eds.; Kluwer Academic Publishers: Dordrecht, 2001.

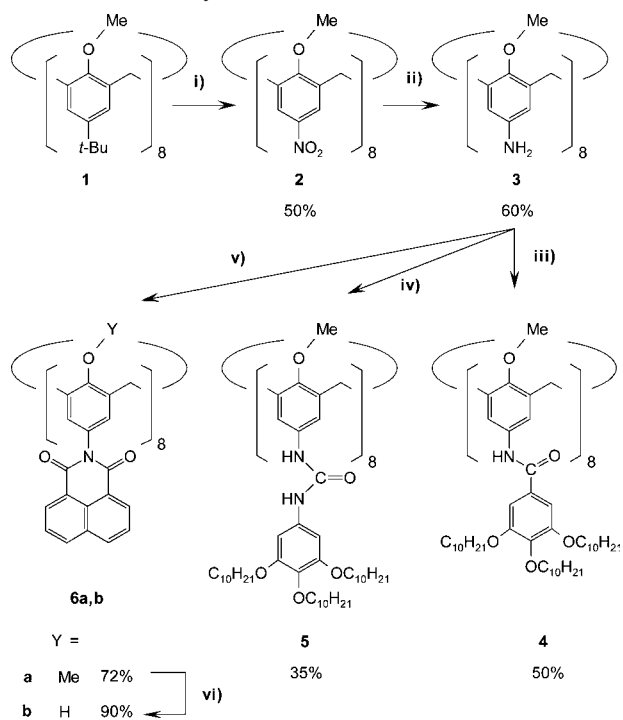
(3) Neri, P.; Consoli, G. M. L.; Cunsolo, F.; Geraci, C.; Piattelli, M. Chemistry of Larger Calix[n]arenes ($n = 7, 8, 9$). In *Calixarenes 2001*; Asfari, Z., Böhmer, V., Harrowfield, J., Vicens, J., Eds.; Kluwer Academic Publishers: Dordrecht, 2001.

(4) (a) Bocchi, V.; Foina, D.; Pochini, A.; Ungaro, R.; Andreetti, G. D. *Tetrahedron* **1982**, *38*, 373–378. (b) Gutsche, C. D.; Lin, L.-G. *Tetrahedron* **1986**, *42*, 1633–1640.

(5) Böhmer, V.; Brusko, V.; Rissanen, K. *Synthesis* **2002**, 1898–1902.

(6) Baudry, R.; Felix, C.; Bavoux, C.; Perrin, M.; Vocanson, F.; Dumazet-Bonnamour, I.; Lamartine, R. *New J. Chem.* **2003**, *27*, 1540–1543.

Scheme 1. Synthesis of Calix[8]arene Derivatives^a



^a Key: (i) HNO_3/AcOH , CHCl_3 , 0 °C, (ii) $\text{NH}_2\text{NH}_2 \cdot \text{H}_2\text{O}$, Pd/C, THF/EtOH, reflux, (iii) $(\text{C}_{10}\text{H}_{21}\text{O})_3\text{C}_6\text{H}_2\text{COCl}$, $(i\text{-Pr})_2\text{NET}$, THF, rt; (iv) $(\text{C}_{10}\text{H}_{21}\text{O})_3\text{C}_6\text{H}_2\text{NCO}$, THF, rt; (v) pyridine, $\text{Zn}(\text{OAc})_2$, reflux; (vi) BBr_3 , CH_2Cl_2 , -70 °C to rt.

with time-averaged D_{4d} symmetry at low temperature (-50 °C) suggest that this conformation also exists in solution. Thus, it should be possible to organize calix[8]arenes into stacked tubular assemblies. For this purpose, we envisaged the introduction of substituents in the para position, which on one hand ensure solubility in apolar organic solvents while they allow on the other hand interactions between the stacked molecules (e.g., via hydrogen bonds or π - π stacking). The covalent connection of these substituents to the calixarene should be rigid but should nevertheless allow a free rotation to reach a suitable distance of the interacting functions. Thus, we explored the synthesis of calix[8]arenes substituted by amide, urea, or imide groups on their wide rim. A recent publication describing water-soluble glucoconjugates of calix[8]arenes⁸ prompts us to report our first results.⁹

The synthetic strategy is outlined in Scheme 1. Ipso nitration of the octamethyl ether **1** (HNO_3/AcOH , 0 °C, CHCl_3) led to its octanitro derivative **2** (50% yield),¹⁰ which was reduced to the octamine **3** by hydrazine in refluxing THF/ethanol in the presence of Pd/C. Acylation of **3** with

(7) Gutsche, C. D.; Gutsche, A. E.; Karaulov, A. I. *J. Inclusion Phenom.* **1985**, *3*, 447–451.

(8) Consoli, G. M. L.; Cunsolo, F.; Geraci, C.; Mecca, T.; Neri, P.; *Tetrahedron Lett.* **2003**, *44*, 7467–7470.

(9) Presented at the 7th International Conference on Calixarenes, Vancouver, 13–18 Aug, 2003.

(10) Under the same conditions, the nitration of the octapropyl-, pentyl-, and -decyl ether was carried out with yields of 43–56%, while CH_2Cl_2 at rt was used in ref 8 for the propyl ether followed by hydrogenation with Pd/C as catalyst.

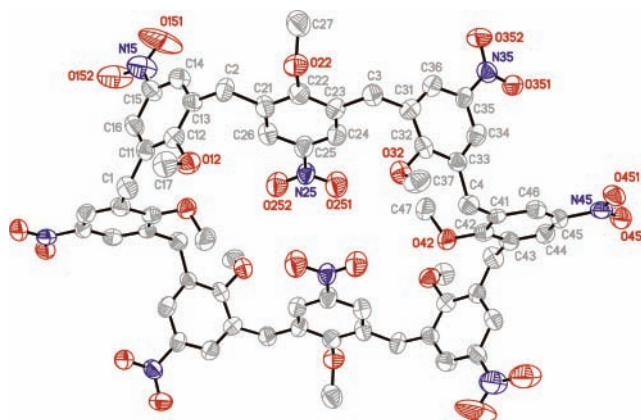


Figure 1. Molecular structure of **2** including the numbering scheme (hydrogen atoms omitted for clarity).

the acid chloride of gallic acid trisdecyl ether ($\text{EtN}(i\text{-Pr})_2$, THF) or the corresponding isocyanate (THF) led to octamides **4** (50%) or octaureas **5** (35%). Reaction with 1,8-naphthalic anhydride (pyridine, $\text{Zn}(\text{OAc})_2$, reflux) gave the octamide **6a** (72%), which could be easily demethylated to **6b** (90%) by BBr_3 (CH_2Cl_2 , -70 °C to rt). All new compounds were characterized by ^1H NMR¹¹ and partly by elemental analysis.

Single crystals of **2** suitable for an X-ray analysis were obtained by slow crystallization from THF.¹²

As found for other octamethyl ethers of calix[8]arenes, the molecule assumes a centrosymmetric conformation (Figure 1). Two nitroanisoole units fill the cavity nearly completely by their nitro groups. Comparison of the torsion angles around the $\text{Ar}-\text{CH}_2-\text{Ar}$ bonds with those found for the octabromo analogue also crystallized from THF reveals differences ranging from 4.8 to 42° with a mean difference of 22.0°. The strong distortion of the macrocycle is also

(11) **Selected NMR Data.** Compound **2**: ^1H NMR ($\text{DMSO}-d_6$, 300 MHz) 7.80 (s, ArH, 16 H), 4.19 (s, ArCH_2Ar , 16 H), 3.66 (s, $-\text{OCH}_3$, 24 H). Compound **4**: ^1H NMR ($\text{THF}-d_8$, 400 MHz) 9.13 (s, $-\text{NH}-$, 8 H), 7.36 (s, ArH, 16 H), 7.10 (s, ArH, 16 H), 3.90 (m, ArCH_2Ar , $-\text{OCH}_2-$, 64 H), 3.47 (s, $-\text{OCH}_3$, 24 H), 1.72 (m under THF, $-\text{OCH}_2\text{CH}_2-$, 48 H), 1.44 (m, $-\text{O}(\text{CH}_2)_2\text{CH}_2-$, 48 H), 1.28 (m, $-\text{O}(\text{CH}_2)_3(\text{CH}_2)_6\text{CH}_3$, 288 H), 0.88 (br t, $-\text{O}(\text{CH}_2)_9\text{CH}_3$, 72 H). Compound **5**: ^1H NMR ($\text{DMSO}-d_6$, 400 MHz, 130 °C) 7.97 (s, $-\text{NH}-$, 8 H), 7.92 (s, $-\text{NH}-$, 8 H), 7.07 (s, ArH, 16 H), 6.66 (s, ArH, 16 H), 3.89 (m, ArCH_2Ar , $-\text{OCH}_2-$, 64 H), 3.45 (s, $-\text{OCH}_3$, 24 H), 1.66 (m, $-\text{OCH}_2\text{CH}_2-$, 48 H), 1.42 (m, $-\text{OCH}_2\text{CH}_2\text{CH}_2-$, 48 H), 1.29 (m, $-\text{O}(\text{CH}_2)_3(\text{CH}_2)_6\text{CH}_3$, 288 H), 0.86 (m, $-\text{O}(\text{CH}_2)_9\text{CH}_3$, 72 H). Compound **6a**: ^1H NMR ($\text{DMSO}-d_6$, 400 MHz, 70 °C) 8.22 (d, ArH, 16 H, $J = 8.3$ Hz), 8.07 (d, ArH, 16 H, $J = 6.8$ Hz), 7.64 (m, ArH, 16 H), 7.02 (s, ArH, 16 H), 4.11 (s, ArCH_2Ar , 16 H), 3.64 (s, $-\text{OCH}_3$, 24 H).

(12) Crystallographic measurement at 100 K using a STOE-IPDS-II diffractometer with graphite-monochromated $\text{Mo K}\alpha$ radiation. Structure solution by direct methods,¹⁴ structure refinement by full-matrix least-squares methods with SHELXL.¹⁵ $\text{C}_{88}\text{H}_{104}\text{N}_8\text{O}_{30}$, $M = 1753.79$, crystal size $0.24 \times 0.22 \times 0.17$ mm³, triclinic, space group $P-1$, $a = 8.8453(16)$ Å, $b = 16.744(4)$ Å, $c = 17.400(4)$ Å, $\alpha = 61.504(15)^\circ$, $\beta = 80.507(16)^\circ$, $\gamma = 74.966(16)^\circ$, $V = 2184.7(8)$ Å³, $Z = 1$, 30 103 reflections, 8038 independent, $R_{\text{int}} = 0.096$, $R_1 = 0.1047$, $wR_2 = 0.2583$ for $I > 2\sigma(I)$. Largest difference peak and hole were 0.480 and -0.368 e/Å³. The crystal was nonmerohedrally twinned (twin matrix: -1 0 0/-0.70 1-0.86/0 0-1). The ratio of the two twin components refined to 0.434(3)/0.566(3). Crystallographic data for the structural analysis have been deposited with the Cambridge Crystallographic Data Centre, CCDC No 224043.

Table 1. Comparison of the Torsion Angles around the Ar-CH₂ Bonds (deg) of **2** with the *p*-Bromo Analogue¹³

	2	<i>p</i> -Br-calix[8]arene octamethyl ether
C42-C41-C4-C33	-95.5	-83.3
C41-C4-C33-C32	163.5	134.6
C32-C31-C3-C23	-77.9	-73.1
C31-C3-C23-C22	-172.0	146.0
C22-C21-C2-C13	172.8	-175.2
C21-C2-C13-C12	80.4	110.3
C12-C11-C1-C43 ^{i a}	-141.0	-164.3
C11-C1-C43 ⁱ -C42 ^{i a}	63.5	86.2

^a Symmetry operator to generate equivalent atoms: (i) $1 - x, 1 - y, 1 - z$.

evident by the distances between opposite *p*-C-atoms which range between 6.0 and 17.4 Å (9.4–16.9 Å for the bromo analogue) (Table 1).

In the crystal lattice (Figure 2), the molecules are arranged to stacks and sheets with π - π contacts between opposite nitroanisoole units.

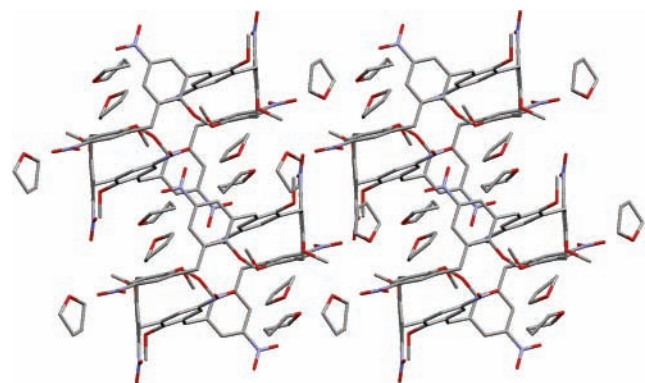


Figure 2. Packing of molecules of compound **2**.

Four of the six included THF molecules lie above and below the macrocycle within a stack while the remaining two fill gaps between molecular stacks.^{14,15}

The ultimate goal was now to prove that the formation of tubular structures due to the peculiar nature of the molecules is feasible. Scanning force microscopy was performed to provide evidence for the assembly of supramolecular structures on surfaces governed by the chemical nature of the calixarene derivatives. Figure 3 shows a typical SFM image of the calix[8]arene derivative **4** self-organized on highly oriented pyrolytic graphite (HOPG) imaged by intermittent contact mode with Q-control.¹⁶ The image clearly reveals that the molecules of octaureas **4** are organized in cylindrical

(13) Bolte, M.; Brusko, V.; Böhmer, V. *Acta Crystallogr.* **2003**, E59, o1691-o1693.

(14) Sheldrick, G. M. *Acta Crystallogr.* **1990**, A46, 467–473.

(15) Sheldrick, G. M. Universität Göttingen, Germany, 1997.

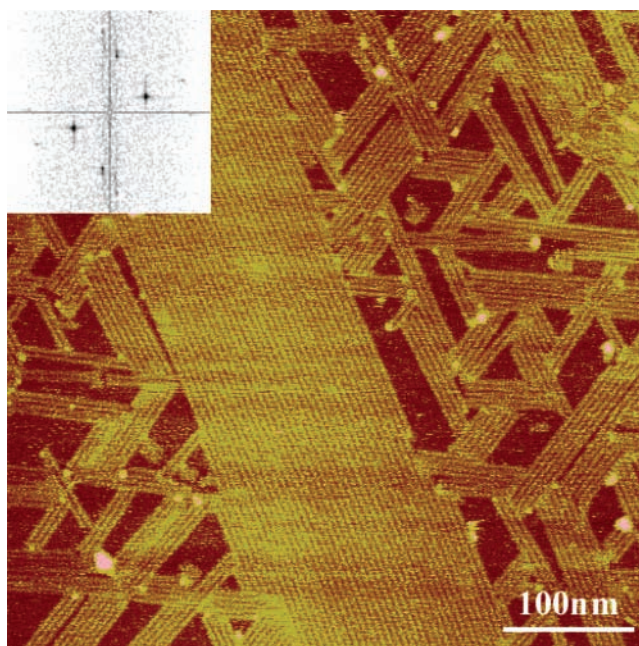


Figure 3. SFM image (TappingMode with Q-control, scan size 550 × 550 nm) of a submonolayer that was prepared by spin casting of a $\sim 10^{-4}$ mg mL⁻¹ solution of **4** in CH₂Cl₂ on HOPG. The 2D power spectrum of the region with densely packed nanorods given in the inset indicates the lateral diameter of nanorods.²⁰

structures. It is evident that parallel nanorods were formed on the graphite surface.

The preparation of the samples by the spin-coating technique¹⁷ renders most of the graphite surface covered with domains consisting of parallel nanorods exhibiting a spacing of 5.2 ± 0.5 nm from section analysis and 5.4 ± 0.2 nm from Fourier analysis (inset of Figure 3). Typically, the domains are 50 nm wide, 50–500 nm long (the longest rod we observed is 1.5 μ m long) and only 1 nm high. Height data from images acquired in the intermittent contact mode might be altered by changes in the viscoelastic properties of the sample, i.e., its softness. Albeit height analysis might be flawed due to indentation of the sample by the tip, the images provide strong evidence that the supramolecular assemblies are indeed the wanted nanotubes composed of stacked calix-

(16) Anczykowski, B.; Cleveland, J. P.; Krüger, D.; Dlings, V.; Fuchs, H. *Appl. Phys. A* **1998**, 66, S885–S889.

(17) Submonolayers of calix[8]arene derivatives were prepared by spin casting. A drop (ca. 10 μ L) of solution was deposited on a freshly cleaved HOPG substrate and the sample was spun at 1000 rpm for 30 s. Calix[8]arene derivatives were dissolved in dichloromethane resulting in a concentration of $\sim 10^{-4}$ mg mL⁻¹ ($(2.1-3.5) \times 10^{-8}$ M). Samples were imaged at room temperature with a commercial SFM (Nanoscope IIIa, Digital Instruments, Santa Barbara, CA) employing TappingMode™ using rectangular silicon cantilevers (Nanosensors, 125 μ m long, 30 μ m wide, 4 μ m thick) with an integrated tip, a nominal spring constant of 42 N m⁻¹, and a resonance frequency of 330 kHz. To control and enhance the range of the attractive interaction regime the instrument was equipped with a special active feedback circuit, called Q-control (Nanoanalytics, Germany) as described in ref 16. The quality factor Q of this oscillating system is increased up to 1 order of magnitude. As a consequence, the sensitivity and lateral resolution are enhanced, allowing us to prevent the onset of intermittent repulsive contact and thereby to operate the SFM constantly in the attractive interaction regime.

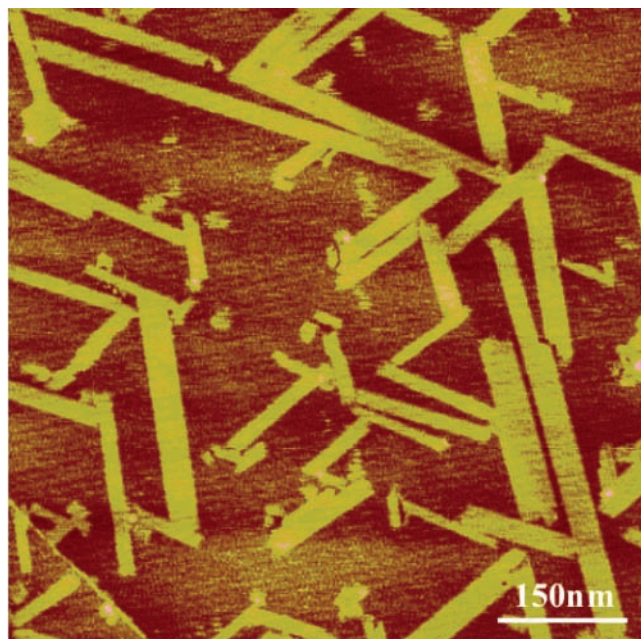


Figure 4. Nanorods cast from a dilute solution ($\sim 10^{-5}$ mg mL $^{-1}$) of **4** in CH $_2$ Cl $_2$ on HOPG.

[8]arenes. Obviously, the domains formed by parallel nanorods are not isotropic since the molecules assemble faster along the long direction of the nanorods than in the direction normal to the rods strikingly displayed by domains consisting of only two or three nanorods (Figure 3). Therefore a nanorod self-assembled from **4** can be called a one-dimensional nanostructure.

The immobilized nanorods were stable and could be imaged by SFM for several hours. Different domains were either oriented parallel (0°) or at an angle of 60° or 120° with respect to each other. The underlying graphite with its hexagonal structure governs this assembly scheme. As a consequence the orientation of the domains of nanorods is determined by the long alkyl chains adsorbing strongly on graphite. Decrease of the calixarene concentration of the spin casting solution results in thinner and shorter domains of nanorods (Figure 4). They were less stable as compared to the highly covered surface and could be curved or even destroyed by the interaction with the AFM tips already after a short scanning time. This implies that the formation of the rods is strongly affected by the lateral interactions of the

neighboring rods. However, the rods formed from a dilute solution (10^{-5} – 10^{-6} mg mL $^{-1}$) still exhibit an elongated shape and sometimes even single nanorods could be found.

One might argue that a thickness of 1 nm would also be explainable by a flat geometry of the molecules with the ring opening parallel to the surface normal rather than a cylinder with the opening of the ring perpendicular to the surface normal. However, a flat geometry could hardly explain the rod formation in particular that of single rods since there is no reason for a preferred assembly direction. This could only be explained by tube formation. The limitation in lateral resolution of the SFM to roughly 1 nm is responsible for the fact that it is not possible to resolve single calixarene monomers if they are closer together than that. This suggests that the periodicity along the nanorod is smaller than 1 nm only explainable by stacking of the individual molecules in a roll of coins fashion with the axis of the cylinder parallel to the surface. Packing of the molecules in this way ensures a distance between the molecules within the rod below 1 nm (~ 0.9 nm) as deduced from the X-ray data. As a consequence, it is highly probable that the calix[8]arene molecules adopt a preferably vertical orientation within the columnar superstructure on the HOPG surface.

Both the assembly of one-dimensional supramolecular assemblies from calix[4]arenes¹⁸ and the formation of the self-assembled monolayers from calix[8]arenes¹⁹ have been observed by others. However, to the best of our knowledge, this is the first description of nanotube formation due to self-assembly of calix[8]arene derivatives on a graphite surface.

Acknowledgment. These studies were supported by BMBF (03N 6500) in the framework of the Center for Multifunctional Materials and Miniaturized Devices.

Supporting Information Available: Experimental procedures for the preparation of compounds **2** to **6**. This material is available free of charge via the Internet at <http://pubs.acs.org>.

OL0361002

(18) Orr, G. W.; Barbour, L. J.; Atwood, J. L. *Science* **1999**, *285*, 1049–1052. Kim, K. S.; Suh, S. B.; Kim, J. C.; Hong, B. H.; Lee, E. C.; Yun, S.; Tarakeshwar, P.; Lee, J. Y.; Kim, Y.; Ihm, H.; Kim, H. G.; Lee, J. W.; Kim, J. K.; Lee, H. M.; Kim, D.; Cui, C.; Youn, S. J.; Chung, H. Y.; Choi, H. S.; Lee, C.-W.; Cho, S. J.; Jeong, S.; Cho, J.-H. *J. Am. Chem. Soc.* **2002**, *124*, 14268–14279.

(19) Pan, G. B.; Liu, J. M.; Zhang, H. M.; Wang, L. J.; Zheng, Q. Y.; Bai, C. L. *Angew. Chem., Int. Ed.* **2003**, *42*, 2747–2751.

(20) The 2D power spectrum displaying two major peaks shows the perfect periodicity of the self-assembled nanorods.